Tectonophysics, 140 (1987) 247–255
Elsevier Science Publishers B.V., Amsterdam – Printed in The Netherlands

On the interpretation of the distinctive pattern of geomagnetic induction observed in northwest India

F.H. CHAMALAUN [1], S.N. PRASAD [2], F.E.M. LILLEY [3], B.J. SRIVASTAVA [2], B.P. SINGH [4] and B.R. ARORA [4]

[1] *Institute of Australasian Geodynamics, Flinders University, Bedford Park, S.A. 5042 (Australia)*
[2] *National Geophysical Research Institute, Uppal Road, Hyderabad 500 007 (India)*
[3] *Research School for Earth Sciences, Australian National University, Canberra, A.C.T. 2600 (Australia)*
[4] *Indian Institute of Geomagnetism, Colaba, Bombay 400 005 (India)*

(Received February 20, 1986; revised version accepted January 13, 1987)

Abstract

Chamalaun, F.H., Prasad, S.N., Lilley, F.E.M., Srivastava, B.J., Singh, B.P. and Arora, B.R., 1987. On the interpretation of the distinctive pattern of geomagnetic induction observed in northwest India. *Tectonophysics*, 140: 247–255.

The geomagnetic variation data from the 1979 Indian array experiment have been reanalyzed and reexamined using the hypothetical event analysis technique. The contour map of the Z/H ratio replicates distinctive anomaly in northwest India previously delineated in maps of the Fourier coefficients. The anomaly reveals the presence of a significant conductor under the Ganga basin. The contour map has been used to derive a response profile perpendicular to the strike of the anomaly, for comparison with 2-D numerical models. An excellent fit was found for a conductor at a depth of 32 km, with a width of 110 km and a conductivity contrast of 1000. This result places the conductor deep within the lithosphere. In the absence of supporting data the origin of the conductor is difficult to resolve. However, it is thought to be related to pressure-released partial melting, caused by fracturing of the Indian crust during the collision of India with Asia.

Introduction

In earlier papers Lilley et al. (1981), Arora et al. (1982) and Srivastava et al. (1984) reported the discovery of a large and distinctive geomagnetic induction anomaly in northwest India. The anomaly was mapped by an array of variometers arranged in four lines perpendicular to the main geological strike of the Himalaya. Figure 1 shows the distribution of variometer sites against the background of the principal geological features. The main anomaly was recorded at the northern sites, while the southern sites showed the possible presence of a second major anomaly in the west. In the previous papers the records were analysed using specific events selected for favourable orientation of the horizontal polarization field. The anomaly was mapped using Fourier transform coefficients, and shown to be present for periods from 20 to 91 min. In Arora et al. (1982) several events per station were averaged and induction arrows computed. These showed a clear reversal in the direction of the induction arrows between the two groups of northerly stations: A1, A2, B1, B2, B3, and C1 in the west and C2, C3, D1, D2, and D3 in the east. The southern stations showed arrows pointing consistently towards a possible second conductor much farther to the west. Of the two anomalies the northerly one is well defined, as it is bracketed by the array and reveals a major

0040-1951/87/$03.50

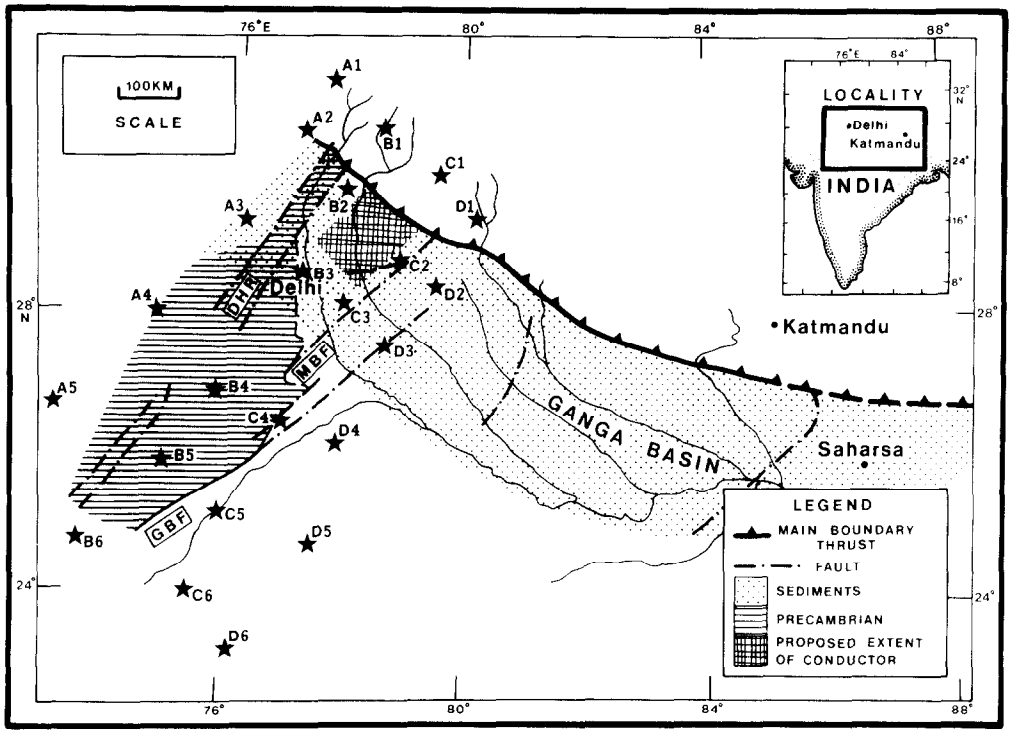

Fig. 1. Showing the distribution of variometer sites of the 1979 array study. *MTF*—main Himalayan thrust zone. Broken lines active lineaments after Valdiya (1976). *DHR*—Delhi–Hardwar Ridge; *MBF*—Muradabad Fault; *GBF*—Great Boundary Fault. Heavily shaded area—possible extend of conductor.

conductor under the Ganga basin. Surprisingly the conductor appears to strike northwards, and perpendicular to the main geological grain defined by the Himalayan suture zone.

Using a line current approximation Lilley et al. (1981) suggested a depth of 100 km or less. Vozoff (1984) reported numerical model studies using the transmission line approach of Madden (Swift, 1971). On the basis of the data reported by Lilley et al. (1981), he concluded that the conductive zone must be 100–200 km wide and that it must have a resistivity of less than 2 Ωm. His depth estimate was 10 km or less.

In this paper we report the results from a reanalysis of the data and a numerical modelling study designed to define in more detail the main shape parameters of the northern conductor as an aid to its geological interpretation. It will be shown that, despite the wide station spacings, the principal parameters can be determined within relatively narrow limits.

Determination of the anomaly profile

For the purpose of numerical modelling it is necessary to obtain the response to horizontal fields which vary perpendicular to the strike of the conductor. The Fourier coefficients, used in earlier papers to map the anomaly, were obtained for particular horizontal field polarizations, not necessarily perpendicular to the strike. The hypothetical event approach of Bailey et al. (1974) has been used here to determine the average response for horizontal fields.

The data used are the same as those reported by Arora et al. (1982). The data comprise only substorm events for all sites. We recomputed the Fourier transforms using a similar approach to that of earlier papers, but included spectral band averaging to get a more stable estimate for the Fourier coefficients. The band averages for several events were used to compute station averages. From these we then computed the transfer functions or induction arrows following Schmucker

(1970) and Everett and Hyndman (1967). The induction arrows are for individual stations and are not corrected for anomalous horizontal variations. We considered that the alternative procedure of selecting a particular station and assuming that it recorded only the normal field, would introduce a comparable error, since such a station cannot readily be identified. The induction arrows are plotted in Fig. 2 and when compared with earlier diagrams (Arora et al., 1982) are seen to be very similar, suggesting that the slightly modified computational procedure did not affect the main result. The transfer functions can now be regarded to represent the average response for each station to varying horizontal fields of any direction.

The required response function may be obtained from the transfer functions by substituting the required direction of the horizontal field and calculating the vertical field response. This is the hypothetical event analysis of Bailey et al. (1974). The main difficulty with this approach is that it assumes a uniform horizontal field.

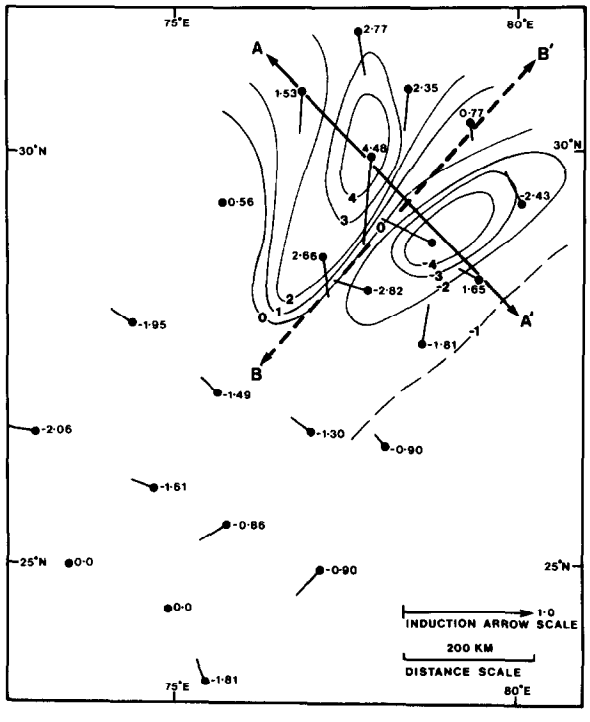

Fig. 2. Contour map of the Z/H ratio for a hypothetical event of horizontal field in the direction $A-A'$. Profile of Fig. 3 is taken along $A-A'$. $B-B'$ presumed strike of conductor. Units are for $H=10$ nT.

For the modelling study, we chose the 53-min period at which the anomaly is best defined and used only the real part of the vertical to horizontal ratio, as the imaginary part is rather small. The resulting contour map of the Z/H ratio for the northwestern part of the array is shown in Fig. 2 together with the induction arrows. It shows, as did the maps of the Fourier coefficients of earlier papers (Lilley et al., 1981; Arora et al., 1982), a well defined anomaly striking north-northeast. The anomaly is characterized by a high near B2 and a distinctive low near C2 some 100 km to the southeast. The contour map also shows closure of the contour lines in the north and south suggesting that the body is 3-D and may not extend much beyond the mapped area. The response profile used in the modelling study was interpolated from the contour map along the line $A-A'$, shown in Fig. 2. The profile is fairly symmetrical with both the positive and negative ratios equal to 0.45. The slope between the maxima and minima is relatively well defined (0.007/km), but that to the west and east of the extrema not. In fact the western slope proved impossible to fit with the models studied below. The half width is about 120 km. Given this width and the large amplitude the anomaly can be expected to be deep and to be caused by a significant conductivity contrast. The maximum to minimum distance is about 165 km and this implies a conductor width of about the same dimension.

Modelling

To model the conductor we used the numerical technique described by Jones and Pascoe (1971). It allows for quite complicated shapes and conductivity structures. Hibbs et al. (1978) obtained encouraging comparisons between the numerical approach and scaled laboratory results, suggesting that the finite difference technique is capable of computing the correct response function, particularly for long periods and moderate resistivity contrasts. The procedure is essentially one of forward modelling: after defining the model and its parameters, the response function is computed and compared with the observed one. The parameters or the model itself are then changed until a

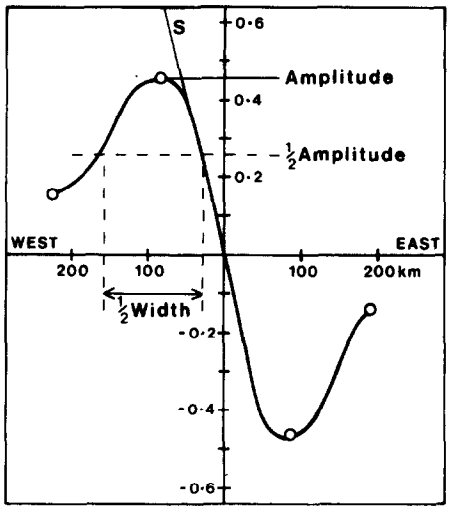

Fig. 3. Profile of observed response along the line $A-A'$ in Fig. 2. The half-width (W') is the horizontal extend of the anomaly at half the amplitude. S is the slope at half the amplitude. Circles represent stations on or close to the profile.

satisfactory fit is obtained. For models with many parameters the convergence can be slow and so, in view of the symmetry of the observed profile, we used a simple model of a tabular body. The Jones and Pascoe (1971) approach involves a grid of variable mesh sizes. Care needs to be exercised in selecting a reasonably uniformly varying grid mesh (Jones and Thompson, 1974). After some experimentation we chose the horizontal grid spacings as shown in Fig. 5. The vertical grid consists of five layers of 1 km followed by the same number of 2, 3, 4, and 5 km and the remainder at 10 km. A total of 75×75 mesh points were used.

In initial tests we assumed a uniform background of $R' = 1000$ Ωm and a tabular body (see Fig. 5) with four parameters: depth to the top (T), thickness (B), width (W) and resistivity (R'). By systematically varying the model parameters we first determined that the model response is not sensitive to changes in B, provided B is comparable to the skin-depth. In subsequent experiments B has, therefore, been kept constant at 50 km. Next we found that the maximum–minimum distance is roughly equal to $W + T$ and that $W = 110$ km fitted the observed profile for a wide range of depth and resistivity values. Keeping B and W constant we then investigated the parameter space in detail by varying T through 18, 30, 42, 52 and 72 km and R' through 1, 2, 3, and 4 Ωm.

To quantify the fit between observed and computed profiles, we noted that the observed profile can be approximated by three characteristics (Fig. 3): the maximum amplitude—which is 0.45; the half width corresponding to the width of the anomaly profile at half the maximum amplitude—which is 120 km; and the slope at the half-width between the extrema—which is 0.007. Using these it is possible to plot nomograms relating each characteristic to the model parameters of depth and resistivity. Examples are given in Fig. 4,

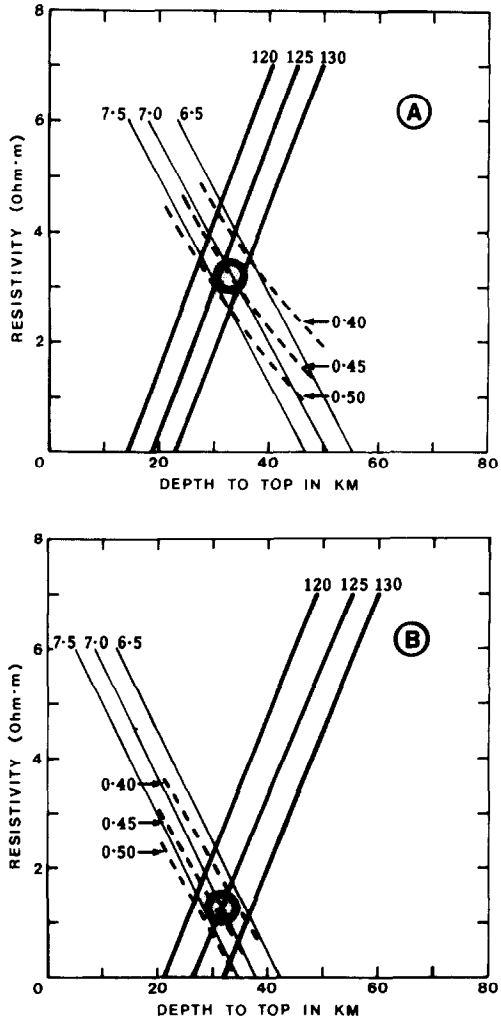

Fig. 4. Nomograms of halfwidth (thick line), slope (thin line) and amplitude (dashed line), as a function of model resistivity and depth to the top. A. For model with uniform background resistivity of 1000 Ωm, but with a conducting layer (A) at the surface. B. The same but with the addition of conducting layers M as shown in Fig. 5.

where only those contours, bracketing the observed values, are shown for the sake of clarity. The nomograms are particularly useful for assessing the range over which the parameters are likely to give an acceptable fit, which ideally should correspond to the intersection of all three contours.

The nomogram for a tabular model with uniform resistivity background of 1000 Ωm, showed that the amplitude and slope contours are more or less parallel and hence do not accurately define the depth or resistivity. On the otherhand, the halfwidth in conjunction with the other two does define an acceptable model within narrow limits. We obtained $T = 42$ km and $R' = 2.0$ Ωm, $W =$ 110 km and $B = 50$ km. The depth to the bottom is not defined, as noted earlier and 50 km is regarded as a minimum.

Next, we investigated the effects of introducing a more realistic background conductivity profile. The background conductivity affects both the diffusion of the field into the subsurface and the actual resistivity of the conductor. The principal difficulty is, however, to choose an appropriate background structure in the absence of any useful data. Since the introduction of each layer adds three further model parameters, we decided to investigate the effects of adding a conductive layer (layer *A* in Fig. 5) at the surface to simulate the presumably more conducting sediments of the Ganga basin, and a conducting layer below the tabular model to represent the conducting mantle (layer *M* in Fig. 5). It was found that both could be subdivided, as detailed below, without affecting the results significantly. Layer *C* represents the bulk of the lithosphere.

Layer *A* was assigned a value of 15 Ωm based on the observed value quoted by Vozoff (1984), and below it was added 10 km of 200 Ωm, which is a reasonable value for the basement (Kaufman and Keller, 1981). The lithosphere has been assigned a value of 1000 Ωm, and layer *M* comprises a layer of 100 km of 100 Ωm, 150 km of 50 Ωm followed by 10 Ωm. The choice of resistivities and thicknesses was from necessity arbitrary. We were guided by the conductivity profile of Drury (1978), which it resembles with slightly higher conductivities and shallower depths to conform to the heat flow values, as discussed below.

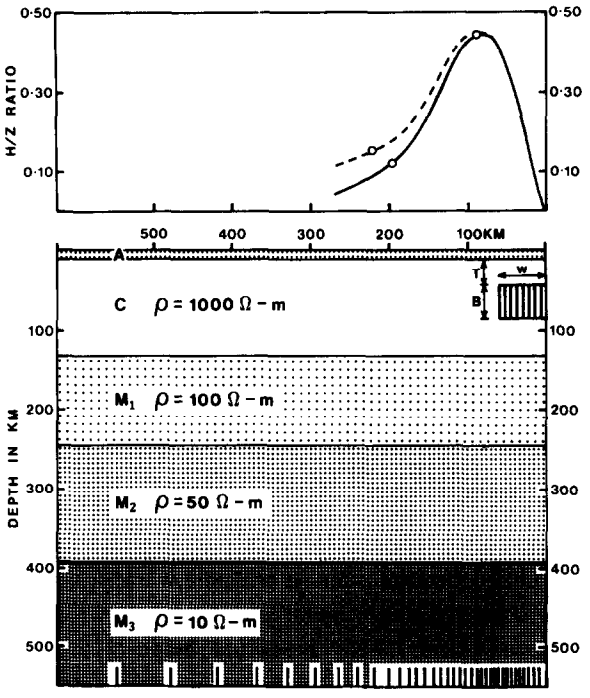

Fig. 5. Final model response compared with the observed response. Model and observed response functions are shown for one half space only. Dashed line for observed curve and solid line for model curve. Between 0 and 100 km the model curve coincides with the observed curve. The model parameters are: *T*—depth to the top; *B*—thickness; *W*—the full width. The subdivisions of the layer *M* into *M1*, *M2*, and *M3* are shown. The vertical short lines at the bottom of the model space represent the horizontal grid-spacings used in the model computations.

In Fig. 4A is shown the nomogram for the case in which layer *A* alone is added, while in Fig. 4B the mantle conductor is also present. The effect of both layers is very similar in that the ratio is reduced, thereby making the conductor appear to be deeper than it is. The important feature to note from a comparison of the two figures, is that the intersection of halfwidth contours with the slope or ratio contours, moves to lower model resistivities as the result of introducing the mantle conductors. Yet the depth to the top of the model is not greatly affected. The intersection of the slope and amplitude contours by itself moves towards greater depths, as do also the halfwidth contours. The two circles in the Fig. 4A and B represent model parameters that yield the same response

curve. That in Fig. 4B represents the final model.

Blohm et al. (1977) and Edwards et al. (1981) have discussed the commonly observed high-conductive layer in the middle to upper crust. It is usually assigned a value of 50 Ωm. We have not succeeded in producing an acceptable model with such a layer included and conclude that a middle crust low resistivity layer is absent under the Ganga basin.

The final model adopted is shown in Fig. 5, where also the observed and computed profiles are compared. Since the model is symmetrical, only one half is shown. Its parameters are: $T = 32$ km, $R' = 1$ Ωm, $B = 50$ km, and $W = 110$ km. It can be seen that the fit is very good considering the uncertainties associated with the observed profile. In particular, the poor fit with the western limb of the observed curve must reflect poor control over the contouring. Also the actual shape of the conductor is unlikely to be accurately represented by a square tabular body. Importantly Fig. 4B clearly shows that the depth to the top, and the resistivity contrast are determined within narrow limits, for the specific background conductivity structure. The width of the conductor cannot be varied by more than a few kilometres, but the depth to the bottom, as noted earlier, is a minimum estimate.

Limitations of the model

The geological interpretation is predicated on this model being valid hence its limitations should be clearly appreciated. The depth is the most important parameter, because it determines the gross geological conditions needed to formulate a geological interpretation. Shallow conductors are more readily explained than deep conductors.

(1) It is assumed that the current profile is indeed a reasonable representation of the true profile. Uncertainties arising from the uniform horizontal field assumption in the hypothetical event analysis, as well as those arising from using only a few events of short duration are probably much less serious than the uncertainty arising from the relatively wide station spacings used in the survey. We have not been able to fit shallow (< 20 km) conductors to the current profile. However, it may well be that profiles of shallow thin-sheet-like conductors, representing perhaps saline beds in the lower Ganga succession, could be generated to pass through the four observed points on the profile. Such profiles would be quite different in the centre portion.

(2) The model parameters are dependent on the background conductivity profile. Changes in depth and corresponding changes in the conductivity contrast would result if a significantly different background structure were to be proposed. Lower crustal depths cannot be ruled out.

(3) The third major uncertainty arises from the lack of data north of the anomaly. The modelling program assumes a conductor of infinite strike length. However, the contour map suggests that the anomaly may not extend much further northward than mapped. It is not clear how 2-D modelling of a 3-D anomaly affects the depth estimate, but using the analogy between line and ring currents one would suspect that 2-D modelling underestimates the depth.

Interpretation

In the following discussion we will assume that the model results indicate a conductor at the crust–mantle interface with a conductivity contrast of 1000 above the background. In a lateral sense the conductor lies just southwest of the main thrust zone of the Himalaya. Stations north of the thrust zone have not recorded a strong continuation of the anomaly, suggesting that it does not continue into the thrust zone itself (Fig. 1). To the south the anomaly falls short of the southern boundary of the Ganga basin. It is entirely contained within the Ganga basin and covered by the several kilometres thick sedimentary sequence contained within the basin. There are several features that like the geomagnetic anomaly trend north, transverse to the strike of the Main Boundary thrust zone. These were discussed in some detail by Valdiya (1976), who showed that many appear to be reactivated faults that existed prior to the collision of India with Asia. The anomaly is situated between two of these (Fig. 1). On the northwest lies the Delhi–Hardwar ridge, which is interpreted as an extension of the Aravalis, plunging under the Ganga basin and to the south-

east lies the Moradabad fault. The anomaly appears to be localized in that the array shows little evidence of another such anomaly to the east or west.

Other geophysical data that might have helped to restrain geological interpretations are scant or ambiguous. The gravity data (Qureshy, 1969; Verma and Subrahmanyam, 1984) show a general decrease over the Ganga basin, entirely consistent with the presence of several kilometres of low-density sediments. The Bouguer gravity map (Verma and Subrahmanyam, 1984) does show an anomaly over the area of the geomagnetic anomaly.

The heat-flow data have been discussed by Gupta (1982) and Singh and Negi (1982), who suggested a general region (Aravalli protocontinent), which includes the geomagnetic anomaly, of high heat flow (40 mW m^{-2}) relative to the Indian subcontinent. The main evidence for high heat flow derives from observations further north and closer to the Himalayan suture zone and to the south in the Aravallis. The implication of the relatively higher than normal heat flow is that the general level of the conductivity in the lithosphere should also be higher. To some extent we have attempted to incorporate this in the model background conductivity. The second implication, noted by Singh and Negi (1982), is that the temperature at the Moho should be higher and they computed the expected temperatures for several models, all of which suggested temperatures as high as 800 °C for the depth corresponding to our conductor. Their models did not, however, include the effects of radiogenic heat, and so are likely to give upper estimates. Gupta's (1982) estimate for the Aravalli craton is 600 °C and his estimate for radiogenic corrected heat flow is 30 mW m^{-2}.

The crustal thickness in India has been summarized by Narain (1973). It appears that much of the Indian sub-continent is underlain by a more or less flat Moho at an average depth of 37 to 40 km (Gupta, 1982), whereas under the Himalaya the depth is between 60 and 70 km. The Moho under the Ganga basin is between 28 and 36 km based on P-wave data (Qureshy, 1969). It is possible that the crust is marginally thinner under the Ganga basin compared to the rest of India. The depth of the conductor determined from the model studies, clearly suggests that it lies almost directly at the Moho boundary with only little penetration into the lower crust.

The seismicity maps (Khatari et al., 1984) show a distinct pattern of enhanced seismicity again broadly coinciding with the area of the anomaly. The seismicity in fact outlines the anomaly quite closely. The main activity is concentrated at the southern and northern ends of the anomaly, with minor activity along the Delhi–Hardwar ridge and Moradabad fault (Kaila and Narain, 1976). The epicentres are shallow and few earthquakes exceed magnitude 5. The fault plane solution for the Moradabad earthquake of August 15, 1966 (Chandra, 1978) showed normal faulting about an east–west strike.

The close proximity of the geomagnetic anomaly to the Himalayan thrust front suggests that the basic origin of the conductor may be related to an upwelling of mantle material into the lower lithosphere. However, the conductivity contrast of 1000 is not readily explained just in terms of a lithological contrast and requires elevated temperatures or more likely partial melting. Partial melting of mantle material has been shown experimentally (Shankland and Waff, 1977; Rai and Manghnani, 1978) to be capable of increasing the electrical conductivity by several orders of magnitude. It is conceivable that local conditions exist conductive to partial melting at a depth of 80 km (1200 °C), corresponding to a dry mantle. However, if water is present the temperature for partial melting is lowered and the depth could well be significantly less (Fyfe, 1976). The factors that control the generation of a partial melt (Chelidze, 1978; Ribe, 1985), and those that control its electrical conductivity (Rai and Manghnani, 1978) are complex and cannot yet be evaluated. Nevertheless we consider it likely that the conductor is due to partial melting at shallow depth in the upper mantle.

It is more difficult to speculate on a mechanism that would have triggered the creation of a rather localized partial melt zone. The proximity to the main Himalayan thrust zone suggests a causal link with the collision process of India with Asia. The associated stress patterns could have resulted in a weakening and fracturing of the lower crust, allowing the upflow of mantle material. The partial

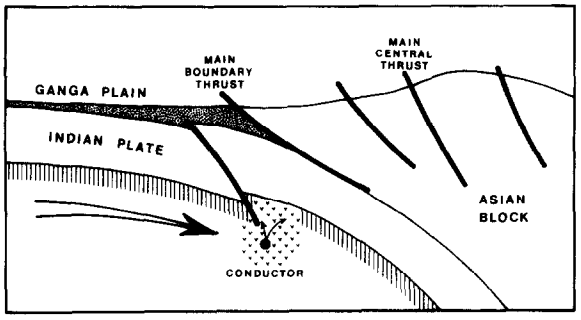

Fig. 6. A schematic drawing showing the possible generation of a conductor as the result of fracturing of the crust under the Ganga basin.

melting would then result from pressure release (Ribe, 1985).

Although the coincidence of the seismicity zones with the proposed conductor boundaries is perhaps fortuitous, it is nevertheless evident that there is considerable present-day tectonic activity associated with the anomaly. It is likely that the seismicity is in response to stresses on the lithosphere and are related to deeper fracture zones. In Fig. 6 we have sketched one possible mode of fracturing that could give rise to the geomagnetic anomaly and which is broadly consistent with the current geophysical data. The diagram attempts to explain the limited north–south configuration of the conductor, and assumes that the east–west limits are similarly controlled by transverse faults such as the Moradabad fault. The structure envisaged implies that triggering of the partial melt resulted from fracturing of the crust above.

Conclusion

The northwest Indian anomaly is one of the largest and most significant continental geomagnetic induction anomalies. The modelling results suggest an upper mantle depth for the anomaly and a very large conductivity contrast. One possible explanation for the latter is by partial melting, which we suggest was initiated by the fracturing of the lithosphere, due to the collision of India with Asia.

To further restrain interpretative models much additional data are required. Geomagnetic variation studies involving a closer spaced array are critically needed to confirm the response function, which in this study was extrapolated over large distances. Such work with magnetic variometers at closer spacings has recently been commenced by Arora and Mahashabde (1985). Also, a real need is for geomagnetic variation data spanning a larger range of frequencies and particularly low frequencies to define the conductivity contrast at depth and the depth to the bottom of the conductor. Equally important, is the need for magnetotelluric depth sounding data to restrain the background conductivity profile in future models. Finally, it would be of considerable interest to examine the propagation of seismic waves through the upper mantle, using tomographic techniques, to confirm the presence of a partial melt.

Acknowledgements

We are indebted to all those people who assisted in the original experiment and were identified in earlier papers. One of us (S.N.P.) is grateful to the Flinders University of South Australia for a short term visiting Fellowship, which enabled him to become familiar with the numerical modelling procedures. We thank Mrs G. Jackson for drafting the figures, so expertly.

References

Arora, B.R., Lilley, F.E.M., Sloane, M.N., Singh, B.P., Srivastava, B.J. and Prasad, S.N., 1982. Geomagnetic induction and conductivity structures in north-west India. Geophys. J.R. Astron. Soc., 69: 459–475.

Arora, B.R. and Mahashabde, M.V., 1985. Transverse conductive structure of northwest Himalayas. Presented at IAGA fifth scientific assembly, Prague.

Bailey, R.C., Edwards, R.N., Garland, G.D., Kutz, R. and Pitcher, D., 1974. Electrical conductivity studies over a tectonically active area in eastern Canada. J. Geomagn. Geoelectr., 26: 125–146.

Blohm, E.K., Worzyk, P., and Scriba, H., 1977. Geoelectrical deep soundings in Southern Africa using the Cabora Bassa power line. J. Geophys., 43: 665–679.

Chandra, U., 1978. Seismicity, earthquake mechanisms and tectonics along the Himalayan mountain range and vicinity. Phys. Earth Planet. Inter., 16: 109–131.

Chelidze, T.L., 1978. Structure sensitive physical properties of partially melted rocks. Phys. Earth Planet. Inter., 17: P41–P46.

Drury, M.J., 1978. Partial melt in the asthenosphere: evidence

from electrical conductivity data. Phys. Earth Planet. Inter., 17: P16–P20.

Edwards, R.N., Bailey, R.C. and Garland, G.D., 1981. Conductivity anomalies: lower crust or asthenosphere? Phys. Earth Planet. Inter., 25: 263–272.

Everett, J.E. and Hyndman, R.D., 1967. Geomagnetic variations and electrical conductivity structure in south-western Australia. Phys. Earth Planet. Inter., 1: 24–34.

Fyfe, W.S., 1976. Chemical aspects of rock deformation. Philos. Trans. R. Soc. London, Ser. A, 283: 221–228.

Gupta, M.L., 1982. Heat flow in the Indian peninsula—its geological and geophysical implications. Tectonophysics, 83: 71–90.

Gupta, R.P. and Bharktya, D.K., 1982. Post-Precambrian tectonism in the Delhi–Aravalli belt, Precambrian Indian shield—evidences from LANDSAT images. Tectonophysics, 85: T9–T19.

Hibbs, R.D., Jones, F.W., Ramaswamy, V. and Dosso, H.W., 1978. Electromagnetic analogue model measurements and finite difference numerical calculations of the response of a conducting slab to three different source fields. Phys. Earth Planet. Inter., 16: 327–340.

Jones, F.W. and Pascoe, L.J., 1971. A general computer program to determine the perturbation of alternating electric currents in a two-dimensional model of a region of uniform conductivity with embedded inhomogeneity. Geophys. J. R. Astron. Soc., 24: 3–30.

Jones, F.W. and Thompson, D.J., 1974. A discussion of the finite difference method in computer modelling of electrical conductivity structures. A reply to the discussion by Williamson, Hewlett and Tammemagi. Geophys. J. R. Astron. Soc., 37: 537–544.

Kaila, K.L. and Narain, H., 1976. Evolution of the Himalaya based on seismotectonics and deep seismic soundings. Proc. Himalayan Geol. Sem. Section II: Structure, tectonics, seismicity and evolution, pp. 1–30.

Kaufman, A.A. and Keller, G.V., 1984. The Magnetotelluric Sounding Method. Elsevier, Amsterdam, 594 pp.

Khatari, K.N., Rogers, A.M., Perkins, D.M. and Algermissen, S.T., 1984. A seismic hazard map of India and adjacent areas. Tectonophysics, 108: 93–134.

Lilley, F.E.M., Singh, B.P., Arora, B.R., Srivastava, B.J., Prasad, S.N. and Sloane, M.N., 1981. A magnetometer array study in northwest India. Phys. Earth Planet. Inter., 25: 232–240.

Narain, H., 1973. Crustal structure of Indian sub-continent. Tectonophysics, 20: 249–260.

Qureshy, M.N., 1969. Thickening of a basalt layer as a possible cause for the uplift of the Himalayas—a suggestion based on gravity data. Tectonophysics, 7: 137–157.

Rai, C.S. and Manghanai, M.H., 1978. Electrical conductivity of ultramafic rocks to 1820 Kelvin. Phys. Earth Planet. Inter., 17: 6–13.

Ribe, N.M., 1985. The generation and composition of partial melts in the earth's mantle. Earth Planet. Sci. Lett., 73: 361–376.

Schmucker, U., 1970. Anomalies of geomagnetic variations in the southwestern United States. Bull. Scripps Inst. Oceanogr., No. 13.

Shankland, T.J. and Waff, H.S., 1977. Partial melting and electrical conductivity anomalies in the upper mantle. J. Geophys. Res., 82: 5409–5417.

Singh, R.N. and Negi, J.G., 1982. High Moho temperatures in the Indian shield. Tectonophysics, 82: 299–306.

Srivastava, B.J., Singh, B.P. and Lilley, F.E.M., 1984. Magnetometer array studies in India and the lithosphere. Tectonophysics, 105: 355–371.

Swift, C.M., 1971. Theoretical magnetotelluric and turam response from two-dimensional inhomogeneities. Geophysics, 36: 38–52.

Valdiya, K.S., 1976. Himalayan transverse faults and folds and their parallelism with subsurface structures of north Indian plains. Tectonophysics, 32: 353–386.

Verma, R.K. and Subrahmanyam, C., 1984. Gravity anomalies and the Indian lithosphere: Review and analysis of existing gravity data. Tectonophysics, 105: 141–161.

Vozoff, K., 1984. Model study for the proposed magnetotelluric (MT) traverse in North India. Tectonophysics, 105: 399–411.